JOURNAL OF BACTERIOLOGY, Aug. 1999, p. 4554–4560 Vol. 181, No. 15
0021-9193/99/$04.00+0

Ni^{2+} Transport and Accumulation in *Rhodospirillum rubrum*

RICHARD K. WATT AND PAUL W. LUDDEN*

Department of Biochemistry, University of Wisconsin-Madison, Madison, Wisconsin 53706

Received 14 October 1998/Accepted 14 May 1999

The *cooCTJ* gene products are coexpressed with CO-dehydrogenase (CODH) and facilitate in vivo nickel insertion into CODH. A Ni^{2+} transport assay was used to monitor uptake and accumulation of $^{63}Ni^{2+}$ into *R. rubrum* and to observe the effect of mutations in the *cooC*, *cooT*, and *cooJ* genes on $^{63}Ni^{2+}$ transport and accumulation. Cells grown either in the presence or absence of CO transported Ni^{2+} with a K_m of 19 ± 4 μM and a V_{max} of 310 ± 22 pmol of Ni/min/mg of total protein. Insertional mutations disrupting the reading frame of the *cooCTJ* genes, either individually or all three genes simultaneously, transported Ni^{2+} the same as wild-type cells. The nickel specificity for transport was tested by conducting the transport assay in the presence of other divalent metal ions. At a 17-fold excess Mn^{2+}, Mg^{2+}, Ca^{2+}, and Zn^{2+} showed no inhibition of $^{63}Ni^{2+}$ transport but Co^{2+}, Cd^{2+}, and Cu^{2+} inhibited transport 35, 58, and 66%, respectively. Nickel transport was inhibited by cold (50% at 4°C), by protonophores (carbonyl cyanide *m*-chlorophenylhydrazone, 44%, and 2,4-dinitrophenol, 26%), by sodium azide (25%), and hydroxyl amine (33%). Inhibitors of ATP synthase (*N*,*N*′-dicyclohexylcarbodiimide and oligomycin) and incubation of cells in the dark stimulated Ni^{2+} transport. ^{63}Ni accumulation after 2 h was four times greater in CO-induced cells than in cells not exposed to CO. The CO-stimulated $^{63}Ni^{2+}$ accumulation coincided with the appearance of CODH activity in the culture, suggesting that the $^{63}Ni^{2+}$ was accumulating in CODH. The *cooC*, *cooT*, and *cooJ* genes are required for the increased $^{63}Ni^{2+}$ accumulation observed upon CO exposure because cells containing mutations disrupting any or all of these genes accumulated $^{63}Ni^{2+}$ like cells unexposed to CO.

Rhodospirillum rubrum expresses a CO oxidation system in response to CO exposure. The CO oxidation system catalyzes the reaction shown in equation 1 (10, 12).

$$CO + H_2O \leftrightarrow CO_2 + H_2 \quad (1)$$

This system contains CO-dehydrogenase (CODH) and a CO-tolerant hydrogenase (4, 12). CODH contains two metal clusters: the active site, Ni-X-Fe_4S_4, and a second Fe_4S_4 cluster involved in electron transfer (19). The CO-tolerant hydrogenase contains a nickel-binding motif conserved in other nickel hydrogenases and requires Ni^{2+} in the growth medium for activity (11). The presence of nickel is essential for the function of the CO oxidation system (4, 12).

The gene encoding CODH (*cooS*) has been cloned, and the operon containing *cooS* has been characterized (21). The CO-oxidation operon (*coo* operon) contains five open reading frames, *cooFSCTJ*. The *cooC* and *cooJ* genes show similarity to genes required for nickel-processing for hydrogenase and urease in other organisms (23). CooC is analogous to the HypB and UreG proteins that have been proposed to hydrolyze nucleotides in order to insert nickel into hydrogenase and urease, respectively (28, 29). CooJ contains a histidine-rich nickel-binding motif that binds four Ni^{2+} atoms per monomer and is similar to UreE and HypB (45). The requirement for CooC and CooJ as nickel-processing proteins was confirmed by mutations that disrupted the reading frames of *cooC* and *cooJ*, resulting in the production of a nickel-deficient CODH (22, 23). The gene products of *cooCTJ* appear to function specifically for nickel insertion into CODH. A mutation disrupting the *cooCTJ* genes exhibits normal levels of the CO-tolerant hydrogenase activity (12).

* Corresponding author. Mailing address: Department of Biochemistry, University of Wisconsin-Madison, 433 Babcock Dr., Madison, WI 53706. Phone: (608) 262-6859. Fax: (608) 262-3453. E-mail: ludden@biochem.wisc.edu.

The mechanism of Ni^{2+} transport and accumulation prior to the insertion of nickel into CODH has not been characterized in *R. rubrum*. To better understand the specific functions of the CooC, CooT, and CooJ proteins, the process of Ni^{2+} transport and accumulation needs to be defined. This includes understanding the mechanism of Ni^{2+} transport and accumulation in the absence of CO when the *cooCTJ* genes are not expressed and in the presence of CO when the *cooCTJ* genes are expressed.

Ni^{2+} transport has been studied in other bacteria, and four classes of Ni^{2+} transport have been reported. The first class is single-component, energy-dependent, high-affinity Ni^{2+} transport system where the K_m for Ni^{2+} is low (17 nM to 5 μM) (7, 20, 25, 47) and Ni^{2+} transport is not inhibited by the presence of other divalent metals (8). The Ni^{2+} transport proteins HoxN, from *Alcaligenes eutrophus* (46), HupN, from *Bradyrhizobium japonicum* (13), UreH, from *Bacillus* TB90 (26), and NixA, from *Helicobacter pylori* (14), have been characterized and have conserved sequence motifs proposed to function in Ni^{2+} binding (14). The second class is the Nik ABCD multicomponent system/transport system from *H. pylori*. This system couples ATP hydrolysis to transport Ni^{2+} (16). The transport systems of *Azotobacter chroococcum* and *B. japonicum* represent a third class of Ni^{2+} transport that requires little or no energy (33, 42). The fourth class of Ni^{2+} transport occurs adventitiously through the Mg^{2+} transport systems of several organisms (8). Maguire and coworkers have characterized three Mg^{2+} transport systems (CorA, MgtA, and MgtB) in *Salmonella typhimurium* (17, 18, 41, 43) and a fourth distinct Mg^{2+} transporter (MgtE) from *Providencia stuartii* and *Bacillus firmus* OF4 (37, 44). CorA, MgtA, and MgtB display different K_m and V_{max} values for transport, are inhibited differently by temperature and divalent metals, and have different mechanisms for transcriptional regulation (34, 38–40). Each Mg^{2+} transport system transports Ni^{2+}, and CorA also transports Co^{2+}. Similar work has been performed with *Escherichia coli* (32). Ni^{2+} transported by Mg^{2+} transport systems

generally has a much higher K_m for Ni^{2+} than the nickel-specific transport systems and is competitively inhibited by Mg^{2+} and other divalent metals (8).

The majority of accumulated Ni^{2+} is found in the form of protein-bound nickel with very little free intracellular nickel (20, 33). The nickel enzymes hydrogenase, urease, CODH, and superoxide dismutase and the F_{430} cofactor of methyl CoM reductase accumulate nickel, as do several accessory proteins required for nickel insertion into these enzymes. Several of these accessory nickel-binding proteins have been purified and characterized. The HypB protein is expressed under hydrogenase-derepressing conditions (30). HypB binds Ni^{2+} and is proposed to assist in the induction of the hydrogenase structural genes (30). Nickel accumulated by HypB is also used for the activation of hydrogenase (30). Maier et al. showed that nickel accumulates in a nickel storage protein and that nickel stored during heterotrophic growth could be used for hydrogenase when cells were derepressed in medium lacking Ni^{2+} (27). A nickel storage role has been proposed for the UreE protein that functions as a nickel-processing protein for urease (5).

The present study demonstrates that Ni^{2+} transport occurs identically in *R. rubrum* grown in the presence or absence of CO. $^{63}Ni^{2+}$ accumulates more rapidly in CO-induced cells due to the accumulation of ^{63}Ni in CODH. CooC, CooT, and CooJ appear to have no role in Ni^{2+} transport but are required for the accumulation of ^{63}Ni in CODH.

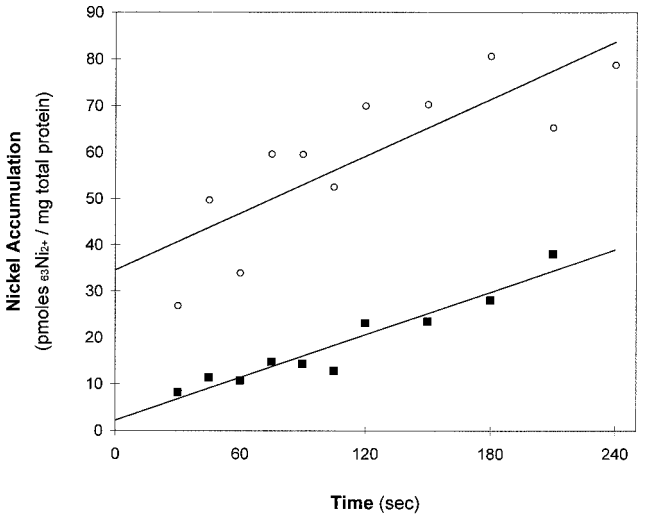

FIG. 1. Initial rate of $^{63}Ni^{2+}$ accumulation by *R. rubrum*. Cells were grown in malate ammonium medium as described in Materials and Methods. Cells were harvested by centrifugation and resuspended in 100 mM MOPS buffer (pH 7.5) (○) or 100 mM MOPS buffer (pH 7.5) containing 1.0 mM $MgCl_2$ (■). The cells were incubated for 30 min at 30°C before the assay was initiated by the addition of 1.0 μM $^{63}NiCl_2$. Nickel accumulated by the cells was measured at the indicated time point by collecting the cells by vacuum filtration, followed by three 5.0-ml washes with 10 mM EDTA in 100 mM Tris buffer (pH 8.0). The filtration assay was as described in Materials and Methods. Each data point represents a single measurement.

MATERIALS AND METHODS

Strains and cultivation. *R. rubrum* UR2 (a spontaneous streptomycin-resistant mutant of *R. rubrum* UR1 [ATCC 11170]) was used as the wild-type strain. The following strains were as described previously and contain insertions into the *cooCTJ* genes that created either polar or nonpolar knockouts of the downstream genes (23). UR469 (UR2 Sm^r Nx^r Gm^r *cooC16*::*aacC1*Ω*linker*) contains an insertion disrupting *cooC* that is polar onto *cooTJ*. UR495 (UR2 Sm^r Nx^r *cooC20*::*linker*) and UR479 (UR2 Sm^r Nx^r *cooT19*::*linker*) contain nonpolar insertions into *cooC* and *cooT*. UR500 (UR2 Sm^r Nx^r Gm^r *cooJ22*::*aacC1*Ω *linker*) contains an insertion into *cooJ*.

R. rubrum strains were cultured in malate ammonium medium with no added nickel (31) in 100-ml vials with rubber stoppers and a gas phase of N_2 at 30°C for 12 to 18 h. Cells were grown in a 30°C warm room 4 in. from a 15-W incandescent light bulb and 6-in. from a 20-W fluorescent bulb. Induction with CO was initiated by adding 20 ml of 99.5% CO gas into the gas phase of the 100-ml vial.

Ni^{2+} transport assay. The Ni^{2+} transport assay used in these studies was a modified version of several previously published Ni^{2+} transport assays (6, 15, 42). *R. rubrum* cell optical density was measured spectrophotometrically at 600 nm (OD_{600}). When cultures reached OD_{600} of 2.0 to 2.5, the culture was collected by centrifugation at 6,000 × *g* for 15 min. The cell pellet was resuspended in 45 ml of anaerobic 100 mM MOPS (morpholinepropanesulfonic acid) buffer at pH 7.5. Cells were transferred (3.0 ml) into anaerobic 20-ml vials with a gas phase of N_2. The cells were incubated at 30°C in an illuminated water bath until Ni^{2+} was added. Controls showed that incubation in MOPS buffer for up to 2 h did not affect the rate of Ni^{2+} transport.

The assay began when 2.8 μCi of $^{63}Ni^{2+}$ ($^{63}NiCl_2$ at 615 mCi/mmol; DuPont NEN Research Products, Inc.) and the indicated amount of unlabeled nickel were added to the cells followed by rapid mixing of the culture (a maximum of 50 μl was added). After being mixed, a sample was removed and vacuum filtered onto a GN-6 Metricell membrane filter (pore size, 0.45 μm; Gelman Sciences, Inc., Ann Arbor, Mich.) at 15 s after Ni^{2+} addition. The GN-6 Metricell membrane filters were previously washed twice with 5.0-ml aliquots of 10 mM $NiCl_2$ in 100 mM MOPS at pH 6.5 to reduce nonspecific binding of $^{63}Ni^{2+}$ to the filter. After the cells were collected on the filter, the cells were washed three times with 10 mM EDTA in 100 mM Tris buffer (pH 8.0) (5.0 ml per wash). With the assistance of the vacuum filtration system, the washing procedure took less than 5 s. The 15-s sample represents rapid binding of $^{63}Ni^{2+}$ to the cell surface and some transport (15) (see also results shown in Fig. 1). The 15-s time point is subtracted from the subsequent time points to calculate the net uptake by the cells. Controls were prepared for each nickel concentration with identical contents but lacking cells to correct for ^{63}Ni binding to the filters.

Additional Ni^{2+} transport experiments were performed with cells that were resuspended in buffer containing 1.0 mM $MgCl_2$ or cells grown in the presence of CO to induce the *coo* operon.

For the studies with inhibitors of Ni^{2+} transport, solvent controls were performed to account for solvents used to solubilize the inhibitors. Filters were transferred to scintillation vials, and Biosafe II scintillation fluid was added (10 ml). ^{63}Ni was detected by liquid scintillation counting by using a ^{14}C setting in a Packard Minaxi Tricarb 4000 series scintillation counter. The protein content of the samples was measured by the method of Lowry et al. (24). Data are expressed as picomoles of Ni^{2+} transported per minute per milligram of total protein.

Nickel accumulation. Cells were grown with illumination, either in the presence or the absence of 20% CO, in a 25-ml volume in 100-ml anaerobic vials with an N_2 gas phase to an OD_{600} of 2.0 to 2.5 in malate ammonium medium. $^{63}Ni^{2+}$ was added to cell cultures to a final concentration of either 100 nM or 1.0 μM (^{63}Ni at 615 mCi/mmol). Samples of the culture were removed at the indicated time points, and cells were collected on a GN-6 Metricell membrane filter as described above for the Ni^{2+} transport assay. CODH activity was monitored by adding cells (1.0 ml) from the indicated time point into a degassed vial with a CO atmosphere (99.5%) containing 10 μl of 0.1 M EDTA to chelate nickel not associated with CODH and 10 μl of 0.1 M methyl viologen. Methyl viologen was added as an electron acceptor for monitoring CODH activity and, in the reduced form, also functioned as an oxygen scavenger. Toluene (20 μl) was added to permeabilize the cells, and the vial containing the sample was placed in a shaking 30°C water bath for 15 min. The sample was then assayed for CODH activity spectrophotometrically by the reported method (9).

Effect of divalent metal ions on Ni^{2+} uptake. Cell culture preparation was identical to that described in the nickel transport assay. The competing divalent metal ion and $^{63}Ni^{2+}$ were added simultaneously to final concentrations of 25 and 1.5 μM (615 mCi/mmol), respectively. The cells were collected and assayed for $^{63}Ni^{2+}$ uptake as described above. A control sample was prepared by adding ^{63}Ni (1.5 μM; 615 mCi/mmol) with no competitive metal.

Effect of metabolic inhibitors on Ni^{2+} uptake. Cell culture preparation was identical to that described in the Ni^{2+} transport assay. The indicated inhibitor was added to the cells, and the cells were incubated for 30 min with illumination at 30°C. The assay was initiated by the addition of $^{63}NiCl_2$ (1.5 μM; 615 μCi/μmol) to the cells. The cells were collected and assayed for $^{63}Ni^{2+}$ uptake as described above. A control sample was prepared by adding $^{63}NiCl_2$ (1.5 μM; 615 mCi/mmol) with no inhibitors present.

RESULTS

Nickel accumulation. The addition of $^{63}NiCl_2$ (1.0 μM, final concentration; 615 mCi/mmol) to *R. rubrum* resulted in the rapid binding of $^{63}Ni^{2+}$ to the cell surface, followed by a linear accumulation of $^{63}Ni^{2+}$. Figure 1 shows the accumulation of $^{63}Ni^{2+}$ in *R. rubrum* in 100 mM MOPS buffer (pH 7.5). The best-fit line represents the accumulation of $^{63}Ni^{2+}$ over a period of 4 min. The line intercepts the *y* axis at 36 pmol of

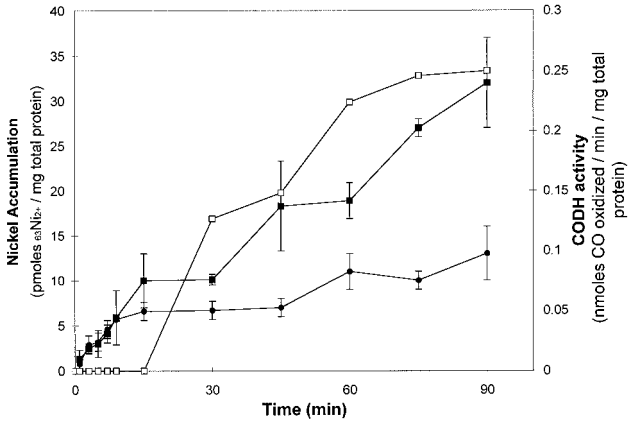

FIG. 2. $^{63}Ni^{2+}$ accumulation in CO-induced *R. rubrum*. CO (20% gas phase) and ^{63}Ni (1 μM; 615 mCi/mmol) were added at the zero time point to *R. rubrum* cells (OD_{600} = 2.0) in malate ammonium medium (■). The control (no CO added) contains ^{63}Ni (1 μM; 615 mCi/mmol) added to *R. rubrum* cells (OD_{600} = 2.0) in malate ammonium medium (●). CODH activity in the cells treated with CO is also indicated (□). The in vitro CODH activity assay is described in the text. Each data point represents the average of two independent measurements. The nickel bound at 15 s was subtracted from the data.

$^{63}Ni^{2+}$/mg of total protein, indicating that a rapid $^{63}Ni^{2+}$ binding phase occurred before the fastest time point measured by this assay (15 s after $^{63}Ni^{2+}$ addition). The rapid binding to the cells occurred when the cells were in buffer or in growth medium, although the binding in growth medium is less due to the presence of molecules that chelate Ni^{2+} (EDTA, phosphate, and malate). Cells that have been killed by heat treatment also exhibit this rapid binding but do not exhibit the linear accumulation (data not shown). The rapid binding of $^{63}Ni^{2+}$ did not occur when $^{63}Ni^{2+}$ was added to *R. rubrum* that had been incubated for 30 min in 100 mM MOPS buffer (pH 7.5) containing 1.0 mM $MgCl_2$. The presence of 1.0 mM $MgCl_2$ did not alter the linear accumulation that follows the rapid binding phase (Fig. 1). A similar experiment was conducted by adding 1.0 μM $^{63}Ni^{2+}$ and 99 μM unlabeled Ni^{2+} to cells and then monitoring the $^{63}Ni^{2+}$ accumulation in the cells. $^{63}Ni^{2+}$ accumulation occurred at a much slower linear rate, and the slope crossed the *y* axis at the zero point, indicating that the unlabeled Ni^{2+} competed with the $^{63}Ni^{2+}$ for both surface binding and for Ni^{2+} transport into the cell (data not shown). In order to distinguish $^{63}Ni^{2+}$ accumulation from surface binding in later experiments, a control sample for rapid binding was used in each assay and subtracted from the subsequent time points to obtain the values representing $^{63}Ni^{2+}$ accumulation.

To determine if exposing the cells to CO at the time of $^{63}Ni^{2+}$ addition induced the production of proteins required for Ni^{2+} transport or accumulation, $^{63}Ni^{2+}$ accumulation experiments were conducted either in the absence of CO or with the simultaneous addition of CO and $^{63}Ni^{2+}$ to a culture. A linear $^{63}Ni^{2+}$ accumulation phase occurred during the first 10 min in the presence or absence of CO (Fig. 2). The first linear accumulation phase is followed by a slower accumulation phase in cells not exposed to CO (Fig. 2). The addition of CO (20%) at the same time as $^{63}NiCl_2$ (1.0 μM, final concentration; 615 mCi/mmol) did not alter the accumulation of $^{63}Ni^{2+}$ during the first 30 min compared to the control. After 30 min of exposure to CO, the accumulation of ^{63}Ni increases dramatically when compared with cells not exposed to CO (Fig. 2). The increase in ^{63}Ni accumulation in the CO-induced culture coincided with the appearance of CODH activity in the culture (Fig. 2). Therefore, the increased accumulation of ^{63}Ni appears to result from the insertion of ^{63}Ni into CODH and perhaps into the CooJ and CooC proteins.

Since apo-CODH the CO-tolerant hydrogenase and CooC, CooT, and CooJ are expressed in CO-induced cells grown on Ni-depleted medium (3, 4, 12, 23), it was possible to examine the accumulation of ^{63}Ni into cells containing apo-CODH and to test the hypothesis that the increased accumulation of ^{63}Ni in CO-treated cultures (Fig. 2) was due to the accumulation of ^{63}Ni into apo-CODH. Apo-CODH can be activated in vivo (in wild-type cells) or in vitro by the addition of nickel (4, 9). All cells in this experiment were grown with nickel-depleted medium and were exposed to CO for 12 h. All cultures expressed similar amounts of apo-CODH, as evidenced by the in vitro activation assay (data not shown). The addition of $^{63}NiCl_2$ to a wild-type culture containing apo-CODH was the positive control for ^{63}Ni accumulation into apo-CODH and other nickel-containing proteins expressed by the CO oxidation system (CO-tolerant hydrogenase and CooJ). The addition of $^{63}Ni^{2+}$ resulted in a linear $^{63}Ni^{2+}$ accumulation phase during the first 15 min. After 15 min a slower, but still significant $^{63}Ni^{2+}$ accumulation phase occurred (Fig. 3). A negative control was the addition of ^{63}Ni to a wild-type culture that was not exposed to CO (Fig. 3). The negative control accounts for the accumulation of $^{63}Ni^{2+}$ by cells not expressing the CO oxidation system. The initial $^{63}Ni^{2+}$ accumulation by the negative control was similar to the CO-induced culture, but the amount of $^{63}Ni^{2+}$ that accumulated after 15 min was much lower (Fig. 3). Mutant strains lacking a functional *cooC* gene are deficient in nickel processing and could not insert nickel into CODH unless a 500 μM nickel concentration was added to the medium (22, 23). The $^{63}Ni^{2+}$ concentration chosen for this experiment (100 nM $^{63}NiCl_2$) was chosen because a mutant in *cooT* grew similarly to wild type in CO-dependent growth experiments (23). At this $^{63}Ni^{2+}$ concentration, no $^{63}Ni^{2+}$ accumulation into apo-CODH will occur in whole cells because Kerby demonstrated that when $^{63}Ni^{2+}$ was added to the *cooC* mutant strain (UR495), no CODH activity was observed (23). A ^{63}Ni

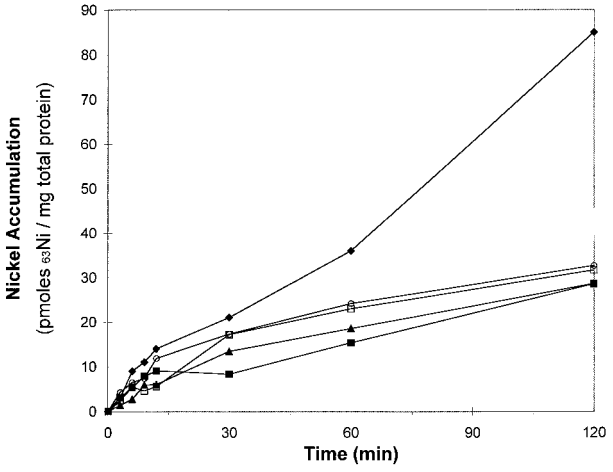

FIG. 3. Nickel accumulation in CO-induced *cooC*, *cooT*, and *cooJ* mutant strains of *R. rubrum*. The cells were grown in malate ammonium medium lacking Ni^{2+} for 12 h with a gas phase of 20% CO–80% N_2 except as indicated. Symbols: ◆, UR2; ■, UR2 without CO (negative control); ▲, nonpolar linker mutation in *cooC* (strain UR495); ○, nonpolar linker mutation in *cooT* (strain UR479); □, mutation in *cooJ* (strain UR500). All cultures except the negative control, which was not CO treated, had similar CODH activities when analyzed by the in vitro Ni^{2+} activation assay. The apo-CODH activation assay was performed on an aliquot of cell culture removed from the culture just prior to the $^{63}Ni^{2+}$ accumulation assay. The nickel bound at time zero was subtracted from the data.

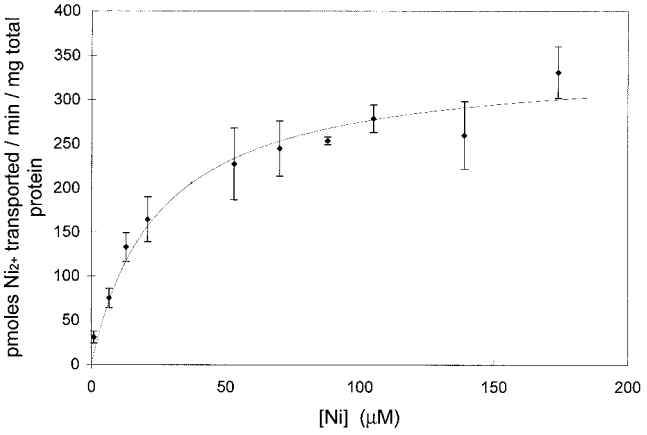

FIG. 4. Kinetics of Ni^{2+} transport by *R. rubrum*. Cells grown in the absence of CO were harvested and resuspended in 100 mM MOPS (pH 7.5) and divided into 12 vials. ^{63}Ni (1.5 μM; 615 mCi/mmol) was added to each vial with the appropriate amount of unlabeled nickel to reach the indicated final nickel concentration. A sample was immediately removed and analyzed for the initial binding of nickel to the cells. Additional samples were removed at 60 and 120 s and then collected by vacuum filtration followed by three 5.0-ml washes of 10 mM EDTA in 100 mM Tris (pH 8.0). The curve represents the mean of data from three independent experiments. Cultures grown in the presence of CO or strains with *cooCTJ* mutationally inactivated and grown with or without CO were also tested for Ni^{2+} transport and produced curves with the same kinetic profiles within the error bars shown (data not shown).

accumulation experiment with a *cooC* mutant strain provided a control that accounted for ^{63}Ni that accumulated in proteins known to bind nickel from the CO oxidation system other than CODH (i.e., CO-tolerant hydrogenase and CooJ). The results in Fig. 2 show that ^{63}Ni accumulation in a *cooC* mutant was similar to the negative control that expressed no CO oxidation proteins. This result indicates that ^{63}Ni accumulation in other CO-induced proteins (i.e., CO-tolerant hydrogenase and CooJ) is very small. ^{63}Ni accumulation assays with mutant strains containing linker mutations disrupting the reading frames of the *cooT* (strain UR479) or *cooJ* (strain UR500) genes also showed ^{63}Ni accumulation that was similar to the negative control (Fig. 3). These data indicate that the observed increase in ^{63}Ni accumulation in the positive control is due to ^{63}Ni associated with CODH. These data also verify that all three of the *cooC*, *cooT*, and *cooJ* gene products must be present for in vivo nickel insertion into CODH to occur under the conditions of this assay.

Kinetics of nickel transport. The linear accumulation of Ni^{2+} during the first 10 min of exposure to $^{63}Ni^{2+}$ shown in Fig. 2 showed saturable kinetics with respect to nickel concentration (Fig. 4). This observation is consistent with Ni^{2+} entering the cell by a transport system. The kinetic data for Ni^{2+} transport by *R. rubrum* grown in the absence of CO was obtained by measuring Ni^{2+} transported at various Ni^{2+} concentrations. The data are consistent with a kinetic uptake system that is saturable with increased Ni^{2+} (Fig. 4). Best-fit calculations with a nonlinear computer fit (Prism Program; Graphpad Graphics, Inc.) showed the K_m for Ni^{2+} to be 19 ± 4 μM with a V_{max} of 310 ± 22 pmol/min/mg of total protein. Similar data were observed when cells were grown in the presence of CO or with a CO-induced mutant strain (UR469) that has a mutation disrupting the *cooCTJ* reading frames. This indicates that the increased accumulation of $^{63}Ni^{2+}$ observed when cells were induced with CO does not occur from the production of a CO-induced Ni^{2+} transport system. Ni^{2+} transport studies were conducted on cells resuspended in buffer containing 1.0 mM $MgCl_2$. The kinetics of Ni^{2+} transport in the presence of $MgCl_2$ are very similar to those without $MgCl_2$. The K_d of 21 ± 4 μM is within the error expected for the transport without $MgCl_2$, and the V_{max} of 252 ± 21 is only 19% lower than the curve without $MgCl_2$. These results indicate that the kinetics of Ni^{2+} transport into the cell in the absence of $MgCl_2$ are a combination of Ni^{2+} being transported by both a Mg^{2+} transporter and a Ni^{2+} transporter. The data also suggest the Ni^{2+} transporter does not require induction by CO or the presence of the CooC, CooT, and CooJ proteins.

Specificity of nickel transport. Mg^{2+} transport systems have been demonstrated to transport Ni^{2+} with lower affinity than Mg^{2+} (8, 34). Ni^{2+}-specific, high-affinity transport systems transport only Ni^{2+} and show very little inhibition from the presence of other divalent metals (8). Table 1 shows the results of nickel transport assays where $^{63}Ni^{2+}$ (1.5 μM) was added simultaneously with 25 μM concentrations of competing divalent metals. The divalent metals commonly tested to determine the specificity of Ni^{2+} transport systems include Mg^{2+}, Mn^{2+}, Zn^{2+}, and Ca^{2+}, and some reports show competition with Co^{2+}, Cu^{2+}, and Cd^{2+}. The results show that Mg^{2+}, Ca^{2+}, Mn^{2+}, and Zn^{2+} did not inhibit Ni^{2+} transport at a 17-fold excess. Mg^{2+} showed only 15% inhibition of $^{63}Ni^{2+}$ transport at a 1 mM concentration (1,000-fold excess; Table 1, Fig. 1, and Fig. 4). The addition of Ca^{2+} actually stimulated $^{63}Ni^{2+}$ transport to a small degree. Co^{2+} inhibited $^{63}Ni^{2+}$ transport 36% at a 17-fold excess (25 μM). Co^{2+} has previously been shown to inhibit nickel-specific transport systems to a slight degree (20). Cu^{2+} and Cd^{2+} showed the most significant inhibition of Ni transport by inhibiting at levels of 66 and 58%, respectively.

Effects of metabolic inhibitors and ionophores. The source of energy required to transport Ni^{2+} can be identified by using inhibitors of metabolic processes and correlating the inhibition of Ni^{2+} transport to the mechanism of the inhibitor. The results for inhibition of Ni^{2+} transport by *R. rubrum* are shown in Table 2. Ni^{2+} transport was completely inhibited by the electron transport inhibitor CN^-. Although no $^{63}Ni^{2+}$ transport occurred in the presence of CN^-, the binding of $^{63}Ni^{2+}$ to the surface of the cells was also decreased fivefold in the presence of CN^- (data not shown). The inhibitory effects of CN^- are most certainly caused by the formation of $Ni(CN)_4^{2-}$. Other electron transport inhibitors, hydroxyl amine and azide, inhibited $^{63}Ni^{2+}$ transport 33 and 25%, respectively. The protonophores CCCP (carbonyl cyanide *m*-chlorphenhydrazone) and DNP (2,4-dinitrophenol) inhibited $^{63}Ni^{2+}$ transport 44 and

TABLE 1. Effect of divalent metals on nickel transport[a]

Metal[b]	Concn (μM)	% of Ni transport[c]
Control (Ni^{2+})	1	100
Ca^{2+}	25	120
Mn^{2+}	25	108
Mg^{2+}	25	95
	1,000	85
Zn^{2+}	25	87
Co^{2+}	25	64
Cd^{2+}	25	42
Cu^{2+}	25	34

[a] The transport assay was performed as described in Materials and Methods. The concentration of ^{63}Ni added to each assay was 1.5 μM (615 mCi/mmol). A data point was taken at 15 s (control for surface binding), 60 s, and 120 s. Cells were collected by filtration, and radioactivity was detected by liquid scintillation counting.

[b] All divalent metal ions were chloride salts.

[c] Percentage of control (no competing metal ion). A 100% value for 1.5 μM $^{63}Ni^{2+}$ is equal to 25 pmol of Ni^{2+}/min/mg of total protein.

TABLE 2. Effect of metabolic inhibitors on nickel transport[a]

Inhibitor	% of Ni transport[b]
Control (no addition)	100
ATPase inhibitors	
DCCD (200 μM)	220
Oligomycin (50 μg/ml)	142
Electron sink/transport	
Sodium azide (1,000 μM)	75
Potassium cyanide (200 μM)	0
Hydroxyl amine (1,000 μM)	67
Protonophores	
CCCP (200 μM)	56
DNP (200 μM)	74
Metal ionophores	
Valinomycin (50 μg/ml)	109
Valinomycin (50 μg/ml) plus 50 mM KCl	154
Nigericin (50 μg/ml)	96
Gramicidin D (50 μg/ml)	165
Miscellaneous	
CO[c]	102
O_2[d]	48
Dark[e]	187
Cold (4°C)	50

[a] Transport assays were performed as described in Materials and Methods. The indicated inhibitor was added to the cells and incubated for 30 min in a shaking 30°C water bath with illumination. Ni^{2+} was added to a final concentration of 1.5 μM, and then the sample was assayed as described in the text.
[b] Percentage of control (100% = 25 pmol of Ni^{2+}/min/mg of protein).
[c] Gas phase was 20% CO and 80% N_2.
[d] Gas phase was air.
[e] Vials containing cells were covered with aluminum foil.

26%, respectively. DNP functions poorly in *R. rubrum* (1), so the effect of protonophores is better represented by the inhibition of CCCP. Incubating the culture in ice for 2 min before the addition of $^{63}Ni^{2+}$ resulted in 50% inhibition of $^{63}Ni^{2+}$ transport. Metal selective ionophores such as valinomycin, nigericin, and gramicidin D did not inhibit $^{63}Ni^{2+}$ transport and, in some cases, stimulated transport. The inhibitors DCCD (*N*,*N*′-dicyclohexyl carbodiimide) and oligomycin also stimulated $^{63}Ni^{2+}$ transport, as did incubating the cells in the dark.

DISCUSSION

This study was undertaken to learn how Ni^{2+} is transported into the cell, to compare Ni^{2+} accumulation in CO-induced cells versus non-CO-induced cells, and to correlate variations in Ni^{2+} transport and accumulation with mutations in the *cooCTJ* genes. The experimental design was intended to increase the understanding of the function of the CooCTJ gene products in *R. rubrum* and to gain an understanding of where nickel processing breaks down in mutants of *cooC*, *cooT*, and *cooJ*.

The initial association of Ni^{2+} with *R. rubrum* occurs as Ni^{2+} binds rapidly to the cell surface (Fig. 1). Incubating the cells in 100 mM MOPS buffer at pH 7.5 containing 1.0 mM $MgCl_2$ for 30 min before the addition of Ni^{2+} stopped the rapid binding of $^{63}Ni^{2+}$ to the cell surface but did not affect Ni^{2+} accumulation by the cells (Fig. 1). The addition of excess unlabeled Ni^{2+} also abolished the rapid binding of $^{63}Ni^{2+}$ to the cells but also significantly slowed the accumulation of $^{63}Ni^{2+}$ in the cells. The binding of $^{63}Ni^{2+}$ to the cell surface has been observed in *Methanobacterium bryantii* (20) and *Methanothrix concilii* (2). Adsorption of Ni^{2+} to *M. concilli* occurs to preparations of purified cell sheaths, and the kinetic data for Ni^{2+} accumulation with purified cell sheath preparations were similar to data obtained for intact cells. These studies concluded that the semispecific cell-surface adsorption was the first step in nickel accumulation by this organism (2).

Nickel transport by *R. rubrum* was a saturable process with Michaelis-Menten-type kinetics over the concentration range of from 1 to 140 μM Ni^{2+}. Analysis of the data by nonlinear regression computer fits indicated that the K_m was 19 ± 4 μM with a V_{max} of 310 ± 22 pmol/min/mg of total protein. The kinetics of Ni^{2+} transport did not change when cells were grown in the presence of CO (20%) or when CO (20%) was added to cells at the time of Ni^{2+} addition to the cells. Therefore, no evidence for a CO-induced nickel uptake system was observed. Ni^{2+} transport was also identical in a CO-induced mutant strain (UR469) that has a mutation disrupting the *cooCTJ* reading frames. This indicates that CooC, CooT, and CooJ are not required for Ni^{2+} transport. Similar Michaelis-Menten saturation kinetics were observed when identical experimental conditions were used with 1.0 mM $MgCl_2$. The data in the absence of Mg^{2+} represents Ni^{2+} transported by the Mg^{2+} transport system, as well as a transport system that is selective for Ni^{2+} versus Mg^{2+}. The kinetic parameters of the Ni^{2+} selective system are better described by the values of K_m = 21 ± 4 and of V_{max} = 252 ± 21 μmol of Ni^{2+}/min/mg of total protein.

Although the Ni^{2+} transport studies reported in the literature differ in assay conditions, some rough comparisons may be made. The K_m of 19 μM for *R. rubrum* is higher than most nickel-specific transport systems reported. The following K_m values have been reported with the following organisms: *M. bryantii*, 3.1 μM (20); *A. kivui*, 2.3 μM (47); *C. thermoaceticum*, 3.2 μM (25), and *A. cylindrica*, 17 nM (7). *B. japonicum* with a K_m of 26 and 50 μM for strains SR and SR470, respectively, has the K_m that most closely approximates the transport by *R. rubrum* (42).

The Ni^{2+} transport system of *R. rubrum* shows selectivity for Ni^{2+} versus the divalent metals Mg^{2+}, Mn^{2+}, Ca^{2+}, and Zn^{2+}. These data are similar to those reported for Ni^{2+} transport in the organisms *Anabaena cylindrica*, *M. bryantii*, *A. kivui*, *C. thermoaceticum*, and *B. japonicum* (7, 20, 25, 42, 47). Co^{2+} and Zn^{2+} show some competitive inhibition to systems labeled as nickel-specific, since these metals inhibited Ni^{2+} transport in *M. bryantii* (Co^{2+}, ~50%) and *B. japonicum* (Zn^{2+}, 46%) (20, 42). Although the Cu^{2+} ion did not affect Ni^{2+} transport in *A. cylindrica* (7), it inhibited Ni^{2+} transport 46% in *B. japonicum* (42) and 64% in *R. rubrum*. Cu^{2+} and Co^{2+} showed levels of inhibition similar to that of the NixA transport system (14).

The energy dependence of Ni^{2+} transport may be established by the use of metabolic inhibitors. Nickel transport has been suggested to occur by energy-independent processes in *Azotobacter chroococcum* (33) and perhaps in *B. japonicum* (42). Ni^{2+} transport required energy in *M. bryantii* and appeared to be coupled to proton movement (20). In *A. cylindrica*, the energy-dependent transport of Ni^{2+} was concluded to rely on the membrane potential (7).

Unfortunately, with *R. rubrum* the effects of metabolic inhibitors were weak and in some cases stimulated Ni^{2+} transport instead of inhibiting it. The electron transfer inhibitors azide and hydroxyl amine showed slight inhibitions of 25 and 33%, respectively. NaN_3 has no effect on photosynthetic phosphorylation, so inhibition by this inhibitor functions at another site (36). The protonophores CCCP and DNP showed mild inhibition of Ni^{2+} transport. The concentration of CCCP used

here completely abolishes photophosphorylation in *R. rubrum*, indicating that the effect of CCCP on Ni^{2+} transport is not as drastic as it is for photophosphorylation (36). These data indicate that a proton gradient may be important in Ni^{2+} transport. Incubation of cells on ice for 2 min inhibited transport 50%, indicating a possible requirement for energy. Metal ionophores that disrupt the membrane potential did not inhibit Ni^{2+} transport, and valinomycin and gramicidin D stimulated transport. The ATP synthase inhibitors DCCD and oligomycin also stimulated Ni^{2+} transport. The stimulation of Ni^{2+} transport by ATPase inhibitors was observed in *A. kivui* grown in the presence of H_2 (47). A possible explanation for the effect of DCCD and oligomycin may be derived from the mechanism of inhibition of these two inhibitors. Both block the flow of protons through the ATP synthase. If protons cannot flow, then the proton gradient increases. This information, coupled with the inhibitory effect of CCCP, indicates that a proton gradient may be involved in Ni^{2+} transport. The stimulation in *A. kivui* was also concluded to result from the effects of the proton motive force (47). Cells that were incubated in the dark also showed stimulated Ni^{2+} transport. Cells that were incubated in the dark and then returned to the light for 1 to 10 min prior to $^{63}Ni^{2+}$ addition also exhibited stimulated Ni^{2+} transport (data not shown). This observation may indicate that incubation in the dark altered the metabolic state of the cells. Since the cells did not return to the original state when exposed to light, it is assumed that an alternate metabolic system is functioning that does not respond like that observed under the original conditions. One possible explanation is that in the absence of light or an energy source, the cells begin to metabolize stored energy sources. Poly-β-hydroxybutyrate is a stored metabolite (35), and the metabolic pathways that convert poly-β-hydroxybutyrate into energy may produce conditions that stimulate Ni^{2+} transport.

The observation that CO-induced $^{63}Ni^{2+}$ accumulation coincided with the appearance of CODH activity in the culture (Fig. 2) suggested that this Ni^{2+} accumulation could function as an assay to monitor Ni^{2+} insertion into CODH. The results show that the majority of the accumulated ^{63}Ni is in CODH and that *cooC*, *cooT*, and *cooJ* gene products are required for in vivo insertion of nickel into CODH (Fig. 3). These results are consistent with CO-dependent growth studies showing that mutants lacking *cooC* or *cooJ* required an increased nickel concentration (100-fold and 10-fold, respectively) before active CODH was produced, allowing CO-dependent growth (23). The CO-dependent growth studies showed that mutants lacking a functional *cooT* gene grew slightly better than the wild type, suggesting that nickel was inserted into CODH in this strain (UR479) (23). No observable nickel accumulation occurred in the *cooT* mutant strain (UR479) under the conditions used in this study. These studies differ in the growth conditions, since the CO-dependent growth studies required growth on CO and were conducted on plates with rich medium. The $^{63}Ni^{2+}$ accumulation studies reported here used a minimal liquid medium and did not require CO-dependent growth.

In conclusion, Ni^{2+} transport occurs by a nickel-selective transport system that can distinguish Ni^{2+} from Mg^{2+}, Mn^{2+}, and Zn^{2+}, and the transport does not depend on the presence of CO. Ni^{2+} transport appears to require energy in the form of a proton gradient. Nickel accumulates both in the absence or presence of CO, and the increased accumulation of nickel is proposed to be from the insertion of ^{63}Ni into CODH. Mutant strains containing mutations disrupting the *cooC*, *cooT*, or *cooJ* reading frames do not show a CO-dependent increase in ^{63}Ni accumulation. The increased accumulation of ^{63}Ni is therefore attributed to ^{63}Ni insertion into CODH, confirming the previous observation that the *cooCTJ* genes are required for nickel insertion into CODH (23).

ACKNOWLEDGMENTS

This work was supported by Department of Energy grant DE-FGO2-87ER13891 to P.W.L.

We thank Robert L. Kerby and Gary P. Roberts for the use of *cooCTJ* mutants constructed by Robert L. Kerby in the lab of Gary P. Roberts.

REFERENCES

1. **Baltscheffsky, M.** 1978. Photosynthetic phosphorylation, p. 595–613. *In* R. K. Clayton and W. R. Sistrom (ed.), The photosynthetic bacteria. Plenum Press, Inc., New York, N.Y.
2. **Baudet, C., G. D. Sprott, and G. B. Patel.** 1988. Adsorption and uptake of nickel in *Methanothrix concilii*. Arch. Microbiol. **150:**338–342.
3. **Bonam, D., L. Lehman, G. P. Roberts, and P. W. Ludden.** 1989. Regulation of carbon monoxide dehydrogenase and hydrogenase in *Rhodospirillum rubrum*: the effects of CO and oxygen on synthesis and activity. J. Bacteriol. **171:**3102–3107.
4. **Bonam, D., M. C. McKenna, P. J. Stephens, and P. W. Ludden.** 1988. Nickel-deficient carbon monoxide dehydrogenase from *Rhodospirillum rubrum*: in vivo and in vitro activation by exogenous nickel. Proc. Natl. Acad. Sci. USA **85:**31–35.
5. **Brayman, T. G., and R. P. Hausinger.** 1996. Purification, characterization, and functional analysis of a truncated *Klebsiella aerogenes* UreE urease accessory protein lacking the histidine-rich carboxyl terminus. J. Bacteriol. **178:**5410–5416.
6. **Bryson, M. F., and H. L. Drake.** 1988. Energy-dependent transport of nickel by *Clostridium pasteurianum*. J. Bacteriol. **170:**234–238.
7. **Campbell, P. M., and G. D. Smith.** 1986. Transport and accumulation of nickel ions in the cyanobacterium *Anabaena cylindrica*. Arch. Biochem. Biophys. **244:**470–477.
8. **Drake, H. L.** 1988. Biological transport of nickel, p. 111–139. *In* J. Lancaster, Jr., (ed.), The Bioinorganic chemistry of nickel. VCH Publishers, Inc., New York, N.Y.
9. **Ensign, S. A., M. J. Campbell, and P. W. Ludden.** 1990. Activation of the nickel-deficient carbon monoxide dehydrogenase from *Rhodospirillum rubrum*: kinetic characterization and reductant requirement. Biochemistry **29:**2162–2168.
10. **Ensign, S. A., and P. W. Ludden.** 1991. Characterization of the CO oxidation/H_2 evolution system of *Rhodospirillum rubrum*. Role of a 22-kDa iron-sulfur protein in mediating electron transfer between carbon monoxide dehydrogenase and hydrogenase. J. Biol. Chem. **266:**18395–18403.
11. **Fox, J. D., Y. He, D. Shelver, G. P. Roberts, and P. W. Ludden.** 1996. Characterization of the region encoding the CO-induced hydrogenase of *Rhodospirillum rubrum*. J. Bacteriol. **178:**6200–6208.
12. **Fox, J. D., R. L. Kerby, G. P. Roberts, and P. W. Ludden.** 1996. Characterization of the CO-induced, CO-tolerant hydrogenase from *Rhodospirillum rubrum* and the gene encoding the large subunit of the enzyme. J. Bacteriol. **178:**1515–1524.
13. **Fu, C., S. Javedan, F. Moshiri, and R. J. Maier.** 1994. Bacterial genes involved in incorporation of nickel into a hydrogenase enzyme. Proc. Natl. Acad. Sci. USA **91:**5099–5103.
14. **Fulkerson, J. F., Jr., R. M. Garner, and H. L. Mobley.** 1998. Conserved residues and motifs in the NixA protein of *Helicobacter pylori* are critical for the high affinity transport of nickel ions. J. Biol. Chem. **273:**235–241.
15. **Grubbs, R. D., M. D. Snavely, S. P. Hmiel, and M. E. Maguire.** 1989. Magnesium transport in eukaryotic and prokaryotic cells using magnesium-28 ion. Methods Enzymol. **173:**546–563.
16. **Hendricks, J. K., and H. L. Mobley.** 1997. *Helicobacter pylori* ABC transporter: effect of allelic exchange mutagenesis on urease activity. J. Bacteriol. **179:**5892–5902.
17. **Hmiel, S. P., M. D. Snavely, J. B. Florer, M. E. Maguire, and C. G. Miller.** 1989. Magnesium transport in *Salmonella typhimurium*: genetic characterization and cloning of three magnesium transport loci. J. Bacteriol. **171:** 4742–4751.
18. **Hmiel, S. P., M. D. Snavely, C. G. Miller, and M. E. Maguire.** 1986. Magnesium transport in *Salmonella typhimurium*: characterization of magnesium influx and cloning of a transport gene. J. Bacteriol. **168:**1444–1450.
19. **Hu, Z., N. J. Spangler, M. E. Anderson, J. Xia, P. W. Ludden, P. A. Lindahl, and E. Münck.** 1996. Nature of the C-cluster in Ni-containing carbon monoxide dehydrogenases. J. Am. Chem. Soc. **118:**830–845.
20. **Jarrell, K. F., and G. D. Sprott.** 1982. Nickel transport in *Methanobacterium bryantii*. J. Bacteriol. **151:**1195–1203.
21. **Kerby, R. L., S. S. Hong, S. A. Ensign, L. J. Coppoc, P. W. Ludden, and G. P. Roberts.** 1992. Genetic and physiological characterization of the *Rhodospirillum rubrum* carbon monoxide dehydrogenase system. J. Bacteriol. **174:** 5284–5294.

22. **Kerby, R. L., P. W. Ludden, and G. P. Roberts.** 1995. Carbon monoxide-dependent growth of *Rhodospirillum rubrum*. J. Bacteriol. **177:**221–2244.
23. **Kerby, R. L., P. W. Ludden, and G. P. Roberts.** 1997. In vivo nickel insertion into the carbon monoxide dehydrogenase of *Rhodospirillum rubrum*: molecular and physiological characterization of *cooCTJ*. J. Bacteriol. **179:**2259–2266.
24. **Lowry, O., N. Rosebrough, A. Farr, and R. Randall.** 1951. Protein measurement with the folin phenol reagent. J. Biol. Chem. **193:**265–275.
25. **Lundie, L. L., Jr., H. C. Yang, J. K. Heinonen, S. I. Dean, and H. L. Drake.** 1988. Energy-dependent, high-affinity transport of nickel by the acetogen *Clostridium thermoaceticum*. J. Bacteriol. **170:**5705–5708.
26. **Maeda, M., M. Hidaka, A. Nakamura, H. Masaki, and T. Ouzumi.** 1994. Cloning, sequencing, and expression of thermophilic *Bacillus* sp. strain TP-90 urease complex in *Escherichia coli*. J. Bacteriol. **176:**432–442.
27. **Maier, R. J., T. D. Pihl, L. Stults, and W. Sray.** 1990. Nickel accumulation and storage in *Bradyrhizobium japonicum*. Appl. Environ. Microbiol. **56:** 1905–1911.
28. **Maier, T., A. Jacobi, M. Sauter, and A. Böck.** 1993. The product of the *hypB* gene, which is required for nickel incorporation into hydrogenases, is a novel guanine nucleotide-binding protein. J. Bacteriol. **175:**630–635.
29. **Moncrief, M. B., and R. P. Hausinger.** 1997. Characterization of UreG, identification of a UreD-UreF-UreG complex, and evidence suggesting that a nucleotide-binding site in UreG is required for in vivo metallocenter assembly of *Klebsiella aerogenes* urease. J. Bacteriol. **179:**4081–4086.
30. **Olson, J. W., C. Fu, and R. J. Maier.** 1997. The HypB protein from *Bradyrhizobium japonicum* can store nickel and is required for the nickel-dependent transcriptional regulation of hydrogenase. Mol. Microbiol. **24:**119–128.
31. **Ormerod, J. G., K. S. Ormerod, and H. Gest.** 1961. Light-dependent utilization of organic compounds and photoproduction of molecular hydrogen by photosynthetic bacteria: relationships with nitrogen metabolism. Arch. Biochem. Biophys. **94:**449–463.
32. **Park, M. H., B. B. Wong, and J. E. Lusk.** 1976. Mutants in three genes affecting transport of magnesium in *Escherichia coli*: genetics and physiology. J. Bacteriol. **126:**1096–1103.
33. **Partridge, C. D., and M. G. Yates.** 1982. Effect of chelating agents on hydrogenase in *Azotobacter chroococcum*. Evidence that nickel is required for hydrogenase synthesis. Biochem. J. **204:**339–344.
34. **Roof, S. K., and M. E. Maguire.** 1994. Magnesium transport systems: genetics and protein structure. J. Am. Coll. Nutr. **13:**424–428.
35. **Sirevåg, R.** 1995. Carbon metabolism in green bacteria, p. 871–883. *In* R. E. Blankenship, M. T. Madigan, and C. E. Bauer (ed.), Anoxygenic photosynthetic bacteria. Klewer Academic Publishers, Dordrecht, The Netherlands.
36. **Smith, L., and P. B. Pinder.** 1978. Oxygen-linked electron transport and energy conservation, p. 641–654. *In* R. K. Clayton and W. R. Sistrom (ed.), The photosynthetic bacteria. Plenum Press, Inc., New York, N.Y.
37. **Smith, R. L., L. J. Thompson, and M. E. Maguire.** 1995. Cloning and characterization of MgtE, a putative new class of Mg^{2+} transporter from *Bacillus firmus* OF4. J. Bacteriol. **177:**1233–1238.
38. **Snavely, M. D., J. B. Florer, C. G. Miller, and M. E. Maguire.** 1989. Magnesium transport in *Salmonella typhimurium*: $^{28}Mg^{2+}$ transport by the CorA, MgtA, and MgtB systems. J. Bacteriol. **171:**4761–4766.
39. **Snavely, M. D., J. B. Florer, C. G. Miller, and M. E. Maguire.** 1989. Magnesium transport in *Salmonella typhimurium*: expression of cloned genes for three distinct Mg^{2+} transport systems. J. Bacteriol. **171:**4752–4760.
40. **Snavely, M. D., S. A. Gravina, T. T. Cheung, C. G. Miller, and M. E. Maguire.** 1991. Magnesium transport in *Salmonella typhimurium*. Regulation of *mgtA* and *mgtB* expression. J. Biol. Chem. **266:**824–829.
41. **Snavely, M. D., C. G. Miller, and M. E. Maguire.** 1991. The *mgtB* Mg^{2+} transport locus of *Salmonella typhimurium* encodes a P-type ATPase. J. Biol. Chem. **266:**815–823.
42. **Stults, L. W., S. Mallick, and R. J. Maier.** 1987. Nickel uptake in *Bradyrhizobium japonicum*. J. Bacteriol. **169:**1398–1402.
43. **Tao, T., M. D. Snavely, S. G. Farr, and M. E. Maguire.** 1995. Magnesium transport in *Salmonella typhimurium*: *mgtA* encodes a P-type ATPase and is regulated by Mg^{2+} in a manner similar to that of the *mgtB* P-type ATPase. J. Bacteriol. **177:**2654–2662.
44. **Townsend, D. E., A. J. Esenwine, J. George, D. Bross, M. E. Maguire, and R. L. Smith.** 1995. Cloning of the mgtE Mg^{2+} transporter from *Providencia stuartii* and the distribution of *mgtE* in gram-negative and gram-positive bacteria. J. Bacteriol. **177:**5350–5354.
45. **Watt, R. K., and P. W. Ludden.** 1998. The identification, purification, and characterization of CooJ. J. Biol. Chem. **273:**10019–10025.
46. **Wolfram, L., B. Friedrich, and T. Eitinger.** 1995. The *Alcaligenes eutrophus* protein HoxN mediates nickel transport in *Escherichia coli*. J. Bacteriol. **177:**1840–1843.
47. **Yang, H. C., S. L. Daniel, T. D. Hsu, and H. L. Drake.** 1989. Nickel transport by the thermophilic acetogen *Acetogenium kivui*. Appl. Environ. Microbiol. **55:**1078–1081.